geosciences

MDPI

Article

Sensitivity Analysis on the Impact of Input Parameters on Seismic Hazard Results: A Case Study of Central America

Carlos Gamboa-Canté [1,*], Mario Arroyo-Solórzano [2], Alicia Rivas-Medina [1] and Belén Benito [1]

[1] Escuela Técnica Superior de Ingenieros en Topografía, Geodesia y Cartografía, Universidad Politécnica de Madrid, 28031 Madrid, Spain; alicia.rivas@upm.es (A.R.-M.); mariabelen.benito@upm.es (B.B.)
[2] Helmholtz Centre Potsdam, GFZ German Research Centre for Geosciences and University of Potsdam, 14473 Potsdam, Germany; marroyo@gfz-potsdam.de
* Correspondence: carlosjose.gamboa@alumnos.upm.es

Abstract: We present a sensitivity analysis on the impact of input parameters and methods used on the results of a probabilistic seismic hazard assessment (PSHA). The accurate estimation of the parameters in recurrence models (declustering and fitting methods), along with the selection of scaling relationships for determining maximum magnitude and the selection of ground motion models (GMMs), enhance control over epistemic uncertainties when constructing the logic tree, minimizing final calculation errors and producing credible results for the study region. This study focuses on Central America, utilizing recent data from seismic, geological, and geophysical studies to improve uncertainty analyses through classic statistical methods. The results demonstrate that proper fitting of the recurrence model can stabilize acceleration variations regardless of the declustering method or *b-value* fitting method used. Regarding scaling relationships, their low impact on the final results is noted, provided the models are tailored to the tectonic regime under study. Finally, it is shown that the GMM contributes the most variability to seismic hazard results; therefore, their selection should be conditioned on calibration with observed data through residual analysis where region-specific models are not available.

Keywords: sensitivity analysis; recurrence parameters; GMM; scaling relationships; seismic hazard; Central America

check for updates

Academic Editor: Ioannis Koukouvelas

Received: 12 November 2024
Revised: 14 December 2024
Accepted: 27 December 2024
Published: 29 December 2024

Citation: Gamboa-Canté, C.; Arroyo-Solórzano, M.; Rivas-Medina, A.; Benito, B. Sensitivity Analysis on the Impact of Input Parameters on Seismic Hazard Results: A Case Study of Central America. *Geosciences* **2025**, *15*, 4. https://doi.org/10.3390/geosciences15010004

Copyright: © 2024 by the authors. Licensee MDPI, Basel, Switzerland. This article is an open access article distributed under the terms and conditions of the Creative Commons Attribution (CC BY) license (https://creativecommons.org/licenses/by/4.0/).

1. Introduction

The inputs that interact to arrive at seismic hazard calculations are subject to uncertainties related to how they are integrated or analyzed in the calculations. For instance, the definitions of seismic sources, recurrence models, seismic parameters, or ground motion models (GMMs) are influenced by uncertainties that have an important impact on the final hazard results. These uncertainties may be *epistemic*, inherent to the models, or *aleatoric*, associated with the standard deviation of the parameters in the models. Logic trees are usually used to control epistemic uncertainties, which integrate possible models for seismic hazard calculations [1,2]. Furthermore, statistical methods can be applied to control the weights of different branches in the logic tree. In this regard, we focused on the sensitivity analysis of different models and input parameters in hazard computations related to the characterization of seismic sources (declustering, fitting method for recurrence model, scaling relationships) and GMMs, taking the Central America (CA) region as a case study. Our aim is to reach a clearer understanding of the uncertainties and to establish a selection guide along with a logic tree weighting proposal replicable in future seismic hazard studies of CA. Based on the sensitivity analysis, an index of the impact of different options (models

and parameters) on the hazard results was obtained. In addition, maps were generated representing the coefficient of variation (CV) of the results for different input options, giving an idea of the zones and conditions that converge to provide more or less robust results. Additionally, we generated a seismic hazard map for peak ground acceleration (PGA) and a return period of 475 years, which was compared with the RESIS II map [3] in order to compare the results of this study with those from a previous regional study based on local seismic data.

2. Seismotectonic Framework

The interactions between the North American, Caribbean, Cocos, and Nazca plates make the tectonic environment of Central America highly active (Figure 1). The boundary between the North American and Caribbean plates gives rise to the Cayman Trough, which is a zone of complex transform faults with a small divergent ridge at its center [4]. This system of transform faults extends westward from the Caribbean, forming the Swan fault (SF), which primarily affects the coasts of Honduras. In Honduras, transtensional fault systems are generated in response to the movement of the Caribbean plate, creating the Honduras Depression (HD) (Figure 1). Additionally, the Guayape fault system (GF), which is the longest and most continuous structure in Honduras, constitutes a complex fault zone ranging from 2 to 25 km in width, oriented N-E, with a length of 290 km [5].

In Guatemala, two sinistral transform fault systems are located in the northern transverse part of the country: the Polochic–Chixoy fault system and the Motagua fault system (PMFS) (Figure 1) [6]. Similarly, to the south of the country lies the beginning of the Central American volcanic arc, the Jalpatagua fault (JF) being a prominent dextral fault with an extension of ~70 km to the Guatemala–El Salvador border [7].

In El Salvador, the northeast movement of the Mid-American Trench (MAT) with respect to the Chortis Block, formed by the North American plate, results in rapid displacement at the point of contact with the regional volcanic arc, leading to the formation of the El Salvador Fault Zone (ESFZ), which is a group of active faults oriented E-W and ESE-WSW, mostly exhibiting strike-slip faulting mechanisms with dextral components and ranging in length from 20 to 30 km [8,9]. Subsequently, the Nicaragua Depression (ND) is formed in the southern region of Nicaragua, this being a prominent geological depression of the late Quaternary, ranging from 40 to 70 km in width and parallel to the Central American volcanic arc (Figure 1), extending ~1000 km from the Nicaragua–Costa Rica border to El Salvador [10].

The subduction of the Cocos plate beneath the Caribbean plate initiates the Mid-American Trench (MAT), which is the most seismically active zone due to its high slip rates from 73.7–76.4 mm/yr in the northwest [6] to 83.0–89.0 mm/yr in the southeast [11], as well as its high rate of seismic events of Mw $\geq$ 4.5, ranging from 5.6 to 12.2 earthquakes per year [12]. Southeast of the trench, an interaction between the Cocos plate and a segment of the Nazca plate forms the Panama Fracture Zone (PFZ), which exhibits dextral strike-slip motion-oriented N-S (Figure 1). Another notable feature in this region is the Cocos Ridge, created by the displacement of the Cocos plate over the Galápagos hot spot, resulting in this bathymetric feature extending over 1000 km in length with a southwest–northeast orientation and an approximate thickness of 25 km, triple the normal thickness of the oceanic crust (Figure 1) [13]. The contact of the Nazca plate with the Caribbean plate forms the Southern Panama Deformed Belt (SPDB), where the oblique motion of the Nazca plate results in this belt being composed of complex faults with shallow seismicity (Figure 1) [14].

Furthermore, in the Caribbean Sea, the Hess Scarp (HE) (Figure 1) represents a fracturing in the bathymetry of the region, starting from Nicaragua [15]. Near this scarp, to the

north of Panama, the North Panama Deformed Belt (NPDB) extends along the coasts of Costa Rica, forming the Central Costa Rica Deformed Belt (CCRDB) (Figure 1) [12].

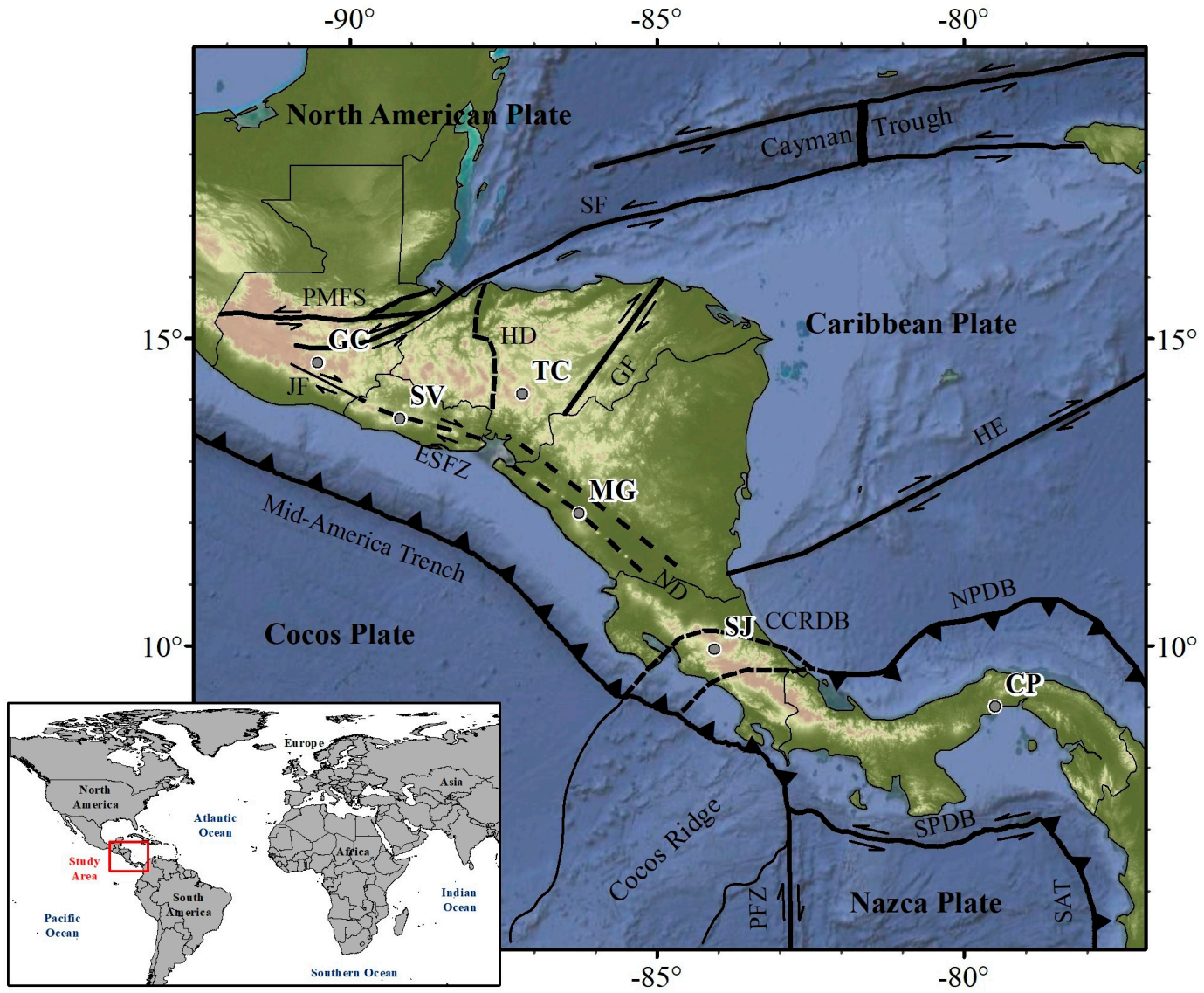


Figure 1. Tectonic framework of Central America. CCRDB—Central Costa Rica Deformed Belt, ESFZ—El Salvador Fault Zone, GC—Guatemala City, GF—Guayape fault, CP—Panama City, HD—Honduras Depression, HE—Hess Scarp, JF—Jalpatagua fault, MG—Managua, ND—Nicaragua Depression, NPDB—North Panama Deformed Belt, PFZ—Panama Fracture Zone, PMFS—Polochic–Motagua fault system, SAT—South American Trench, SF—Swan fault, SJ—San Jose, SPDB—South Panama Deformed Belt, SV—San Salvador, TC—Tegucigalpa.

3. Seismic Hazard Assessment

3.1. Earthquake Catalog

We used the updated regional earthquake catalog of Central America generated from 14 databases of local and regional seismic networks as part of the results of the KUK-AHPÁN project. This earthquake catalog comprises 260 548 seismic events ranging from Mw 1.0 to 7.9 and of depths up to 300 km in the period from 1520 to 2020 [16]. Figure 2 shows the seismicity map used in this study derived from the regional earthquake catalog for seismic events of more than Mw 3.0.

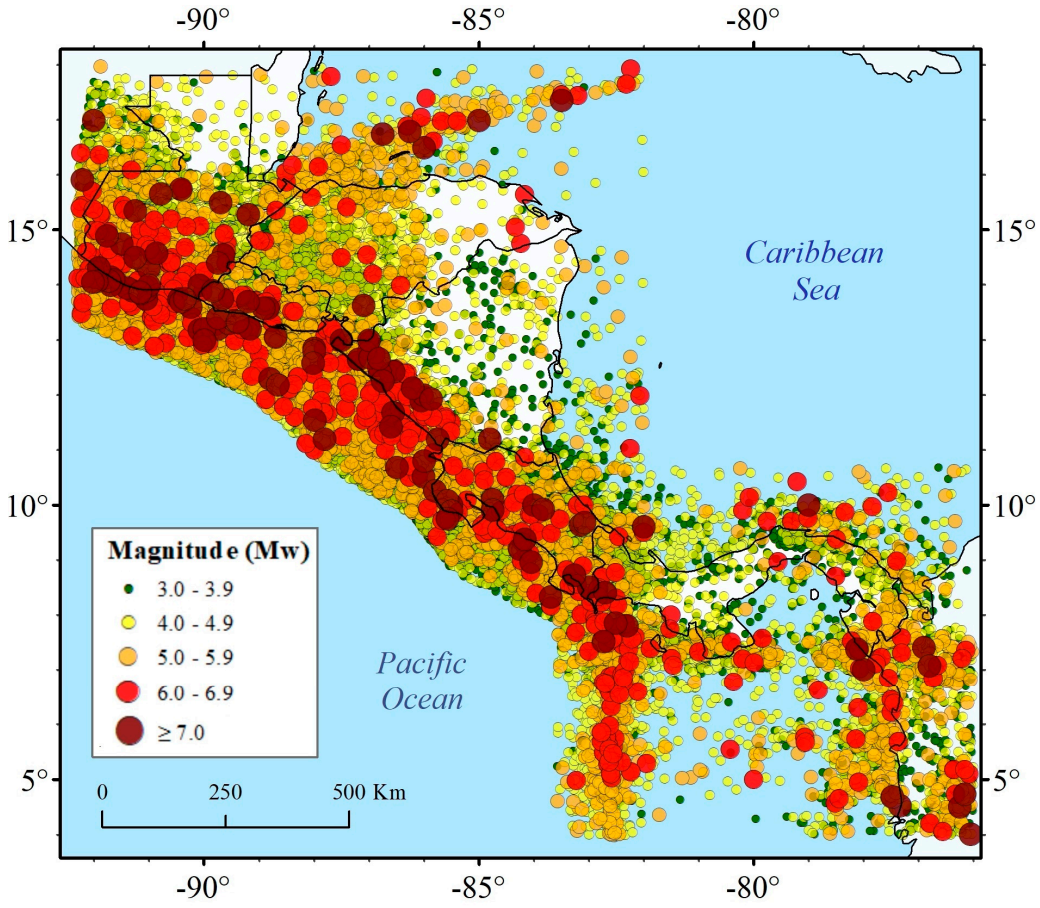


Figure 2. Regional earthquake catalog for Central America in 1520–2020 [16].

Since the earthquake catalog covers a period of 500 years, it was necessary to conduct a temporal completeness analysis for the different magnitude ranges. This analysis evaluates variations in magnitude ranges over time to identify the periods during which earthquakes were considered to have been completely recorded. Gamboa-Canté et al. (2024) [16] performed this analysis using the method proposed by Stepp (1972) [17], which examines the cumulative percentage of seismic events [%N(m)] for different magnitude ranges (Mw). By visually inspecting the slope increases in the cumulative percentages, researchers identify periods where data recording becomes complete, marking these as completeness periods. Table 1 presents the reference tears that mark the period of completeness for each magnitude range proposed by Gamboa-Canté et al. (2024) [16].

Table 1 indicates that it is not possible to reliably determine the completeness periods for magnitudes Mw < 3.0. This is because detecting seismic events of such magnitudes only began in the late 1990s, and local seismic agencies in each country continue to enhance the density and coverage of seismic networks to detect these events [16]. Conversely, most seismic events with magnitudes Mw $\geq$ 7.5 are historical records not captured during the instrumental period, complicating the determination of complete recording periods for these events. The seismicity rates are determined taking into account these reference years and the periods where the earthquake catalog is complete for each magnitude range.

Table 1. Reference years marking the beginning of the period of completeness for each magnitude range for the regional earthquake catalog of Central America.

Magnitude Range (Mw)	Percentage of Cumulative Seismic Events [%N(m)]
Mw < 2.0	¿2005?
2.0–2.4	¿2000?
2.5–2.9	¿1995?
3.0–3.4	1992
3.5–3.9	1992
4.0–4.4	1985
4.5–4.9	1975
5.0–5.4	1963
5.5–5.9	1950
6.0–6.4	1915
6.5–6.9	1900
7.0–7.4	1830
7.5–7.9	¿1765?

3.2. Characterization of the Seismic Sources

We employed the seismic zoning proposed by Alvarado et al. (2017) [12] to characterize the zone-type seismic sources in the region. This zoning is an update of the proposal by Benito et al. (2012) [3] in the RESIS II project, where seismic zones in the more recent zoning model were defined through a comprehensive analysis of geological, geodetic, and seismological information from the region. These seismic zones are distributed as follows: (1) 41 seismic sources in the upper plate regime extending up to a depth of 25.0 km (Figure 3a), (2) 10 seismic sources in the interface regime ranging from depths of 10.0 to 40.0 km (Figure 3b), and (3) 7 seismic sources in the inslab regime with depths exceeding 40.0 km (Figure 3b).

An important characteristic of the Alvarado et al. (2017) [12] zoning is the changes introduced in the subduction with respect to other previous zoning models [3]. The angle of subduction along the Mid-American Trench (MAT) varies significantly across Central America, influencing both the depth and characteristics of seismicity in the region. In Guatemala, a steeper subduction angle allows earthquakes to reach depths of up to 250 km, while in Costa Rica, a shallower angle restricts seismic events to a maximum depth of approximately 70 km [12]. This variation results in a segmented subduction zone, with each segment potentially experiencing differences in the frequency and magnitude of large earthquakes. Additionally, in southern Panama, where the Nazca plate converges at an oblique angle with a shallow subduction dip of less than 20°, seismic activity is predominantly shallow (less than 20 km) but capable of generating events of significant magnitude. These differences in the subduction angle not only shape the regional distribution of seismicity but also impact focal mechanisms and potential energy release across the tectonic boundaries of Central America [12].

This model represents a consensus among Central American seismologists, avoiding national boundary discontinuities and fostering a regional approach to seismic risk management [12]. This regional integration of seismic, tectonic, and GPS data has enabled a more precise demarcation of seismic zones, supporting a probabilistic seismic hazard analysis across the region.

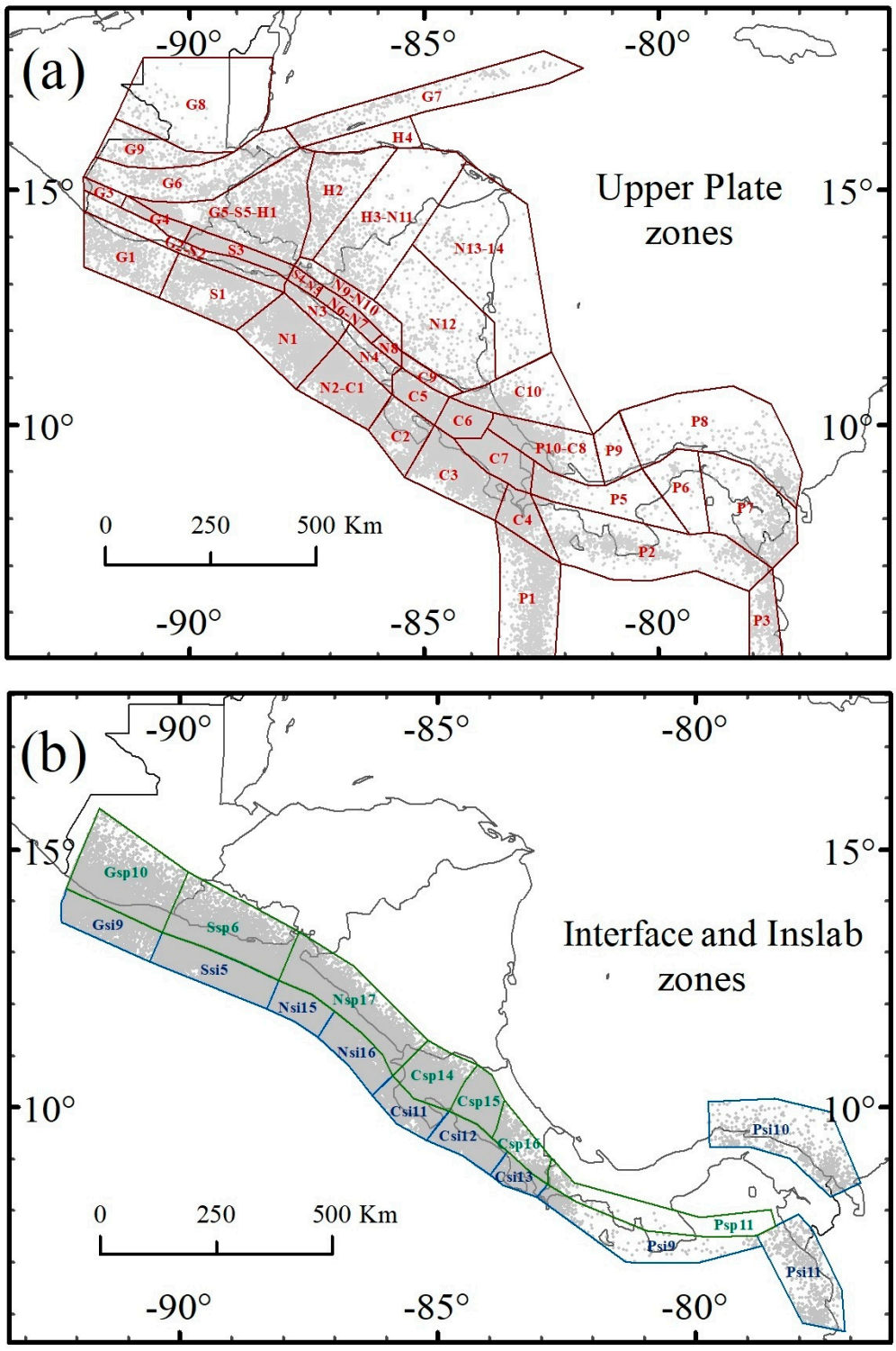


Figure 3. Seismic zones for Central America proposed by Alvarado et al. (2017) [12] for the (**a**) upper plate zones (red color), (**b**) interface zones (blue color), and inslab zones (green color). Gray dots represent the spatial distribution of seismicity within each seismic zone.

3.3. Ground Motion Models (GMMs)

Ground Motion Models (GMMs) significantly influence the acceleration outcomes in seismic hazard calculations. Therefore, it is preferable to develop GMMs specific to the study area. However, until a suitable model for CA is developed and calibrated, we need to identify the most suitable GMMs among those published in the specialized literature.

The most effective way to analyze and identify the most suitable GMMs for a given region is by conducting a residual analysis, measuring the difference between the predicted and observed acceleration values in the region. This approach aims to determine which GMM best characterizes the attenuation in the region [2]. In national-level seismic hazard studies for El Salvador and Costa Rica, several GMMs have already been identified as those which best fit to the observed data [18,19]. These studies employed two approaches: the Log-likelihood (LLH) approach proposed by Scherbaum et al. (2009) [20], and the ranking approach based on Euclidean Distance (EDR) proposed by Kale and Akkar (2013) [21]. In this regard, we have taken the calibrated GMMs from these two national studies to be used in this regional study.

For the upper plate regime, we selected the GMMs of Kanno et al. (2006) [22], Atkinson and Boore (2011) [23], Akkar et al. (2014) [24], Boore et al. (2014) [25], and Cauzzi et al. (2015) [26]. In the interface regime, we selected the models proposed by Youngs et al. (1997) [27], Kanno et al. (2006) [22], Zhao et al. (2006) [28], and Abrahamson et al. (2016) [29]. Lastly, in the inslab regime, the models proposed by Youngs et al. (1997) [27], Kanno et al. (2006) [22], Abrahamson et al. (2016) [29], and Montalva et al. (2017) [30] were selected.

3.4. Sensitivity Analysis of Methods, Models, and Input Parameters in the Seismic Hazard Results

A sensitivity analysis helps to control the variability that the results of seismic hazard calculations may exhibit due to the epistemic uncertainty of the models applied to define the input parameters or the aleatory errors [1,2]. These sensitivity analyses can be conducted using classical statistical methods, where the results allow a clearer understanding of the variability of the hazard results for different calculation options in a logical tree, thus showing the epistemic uncertainty [31–33].

We developed this sensitivity analysis through the evaluation of the coefficient of variation (CV), which indicates the degree of variability in the hazard results and is defined as follows:

$$\mathrm{CV} = \frac{\sigma}{\overline{x}} \quad (1)$$

where σ is the standard deviation of the set of results being analyzed and $\overline{x}$ the mean value of those results. Some authors suggest that for low CV values (<0.15), data dispersion is considered insignificant, resulting in a homogeneous behavior of the calculation options or models handled. In contrast, higher CV values ($\geq$0.15), represent a notable dispersion of the results depending on the options followed and are therefore not very robust results in the areas where these high CV values are present [32,34].

The sensitivity analysis was focused on evaluating the impact on the results of the following inputs and methods integrated into the seismic hazard calculations: (1) declustering methods, (2) methods for fitting the recurrence models (*b-value* and *a-value*), (3) scaling relationships for estimating Mmax, and (4) application of different GMMs.

3.4.1. Declustering Method

Time-independent seismic hazard analysis based on Poissonian models assumes that earthquake occurrence within a given time period and a certain zone is random. To apply these models, the earthquake catalog must contain independent seismic events over time and space, requiring the removal of those considered *dependent seismicity* (e.g., aftershocks, foreshocks, and swarms) through declustering methods.

The declustering of the earthquake catalog, depending on the method used, will result in variations in the calculations of seismic source parameters [35–37]. In this paper, we used two declustering methods for this analysis: (1) the Reasenberg (1985) [38] declustering method (RSB), which employs an algorithm to group seismic events in an interaction zone, analyzing events considered aftershocks based on their spatiotemporal location; and (2) the

spatiotemporal window-based method by Gardner and Knopoff (1974) [39] and modified by Uhrhammer (1986) [40] (UHR), identifying distance and time windows according to the magnitude of the main event to remove aftershocks. These two declustering methods were selected because they are the most widely used in the Central American region for seismic hazard studies [3,18,41–43].

The RSB method was applied using the ZMAP program developed by Wiemer (2001) [44], while the UHR algorithm was executed using the Hazard Model Toolkit [45] included in the OpenQuake program developed by the Global Earthquake Model Foundation (GEM) [46,47]. The sensitivity analysis of these two declustering methods in the hazard results was performed in conjunction with the method for fitting the recurrence model explained in the following section.

3.4.2. Estimation of Recurrence Parameters

The recurrence model used in the seismic sources was based on the recurrence model proposed by Gutenberg and Richter (1944) [48]. We used two fitting methods in the recurrence models, (1) least squares (bLS) and (2) maximum likelihood (bML), proposed by Aki (1965) [49], along with the completeness analysis defined by Weichert (1980) [50].

We then calculated the coefficient of variation (CV) to understand the spatial variability in the hazard results for the upper plate, interface, and inslab regimes using different combinations of the declustering–fitting methods: (1) RSB-bLS, (2) RSB-bML, (3) UHR-bLS, and (4) UHR-bML. Figure 4 shows the CV map in the analyzed tectonic regimes.

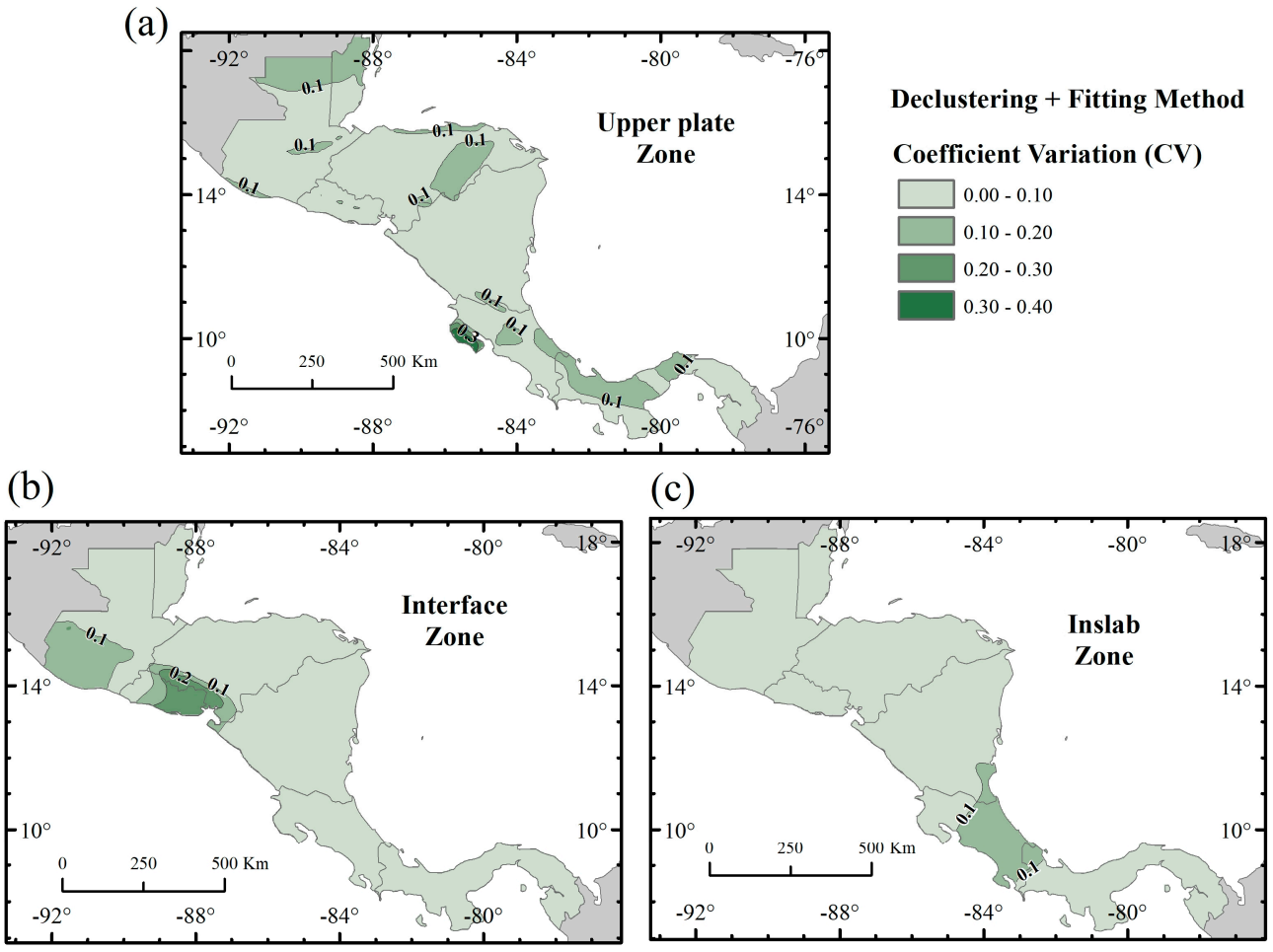


Figure 4. Variability related to recurrence parameters and declustering method for the (**a**) upper plate zone, (**b**) interface zone, and (**c**) inslab zone.

In most of the seismic zones of the upper plate, interface, and inslab regimes, the variability was very low (CV $\leq$ 0.10) (Figure 4). However, there were some zones with greater variation in acceleration (CV > 0.10), e.g., in the upper plate regime of the Backarc zone of north Guatemala (G8) and Honduras (H4; H3-N11), the Forearc zone of Costa Rica (C2), and the volcanic arc zones of Panama (P5; P6) (Figure 4a). In the case of the interface regime, this was found in the zones of Guatemala (Gsi9), El Salvador (Ssi5), and the Gulf of Fonseca (Nsi15) (Figure 4b). Finally, the inslab regime showed a high CV in the transition region of the Costa Rica and Panama subduction (Csp15, Csp16) (Figure 4c).

According to the results obtained, the low CV values (CV < 0.10) in most areas of Central America indicate a consistency in the accelerations calculated under the different combinations of the declustering and fitting methods for the recurrence parameters. This indicates the stability of the accelerations predicted by the different combinations. This implies that the earthquake recurrence rate in these areas is relatively stable and predictable, regardless of the declustering method and fitting method used.

For areas with a relatively high coefficient of variation (CV > 0.10), various factors may contribute, depending on the seismotectonic context of each zone. For instance, the Backarc zones of Guatemala (G8) and Honduras (H4; H3-N11) are characterized by low seismic activity, with a predominance of earthquakes of magnitudes Mw $\leq$ 5.5. When data are applied using declustering methods, the latter can condition the recorded seismic activity in these low magnitudes, affecting the calculation of the recurrence parameters. Additionally, the lack of records of these low-magnitude earthquakes in the earthquake catalog can significantly impact the *b-value* fitting method.

A similar situation occurs in the Forearc zone of Costa Rica (C2) and the interface zone of El Salvador (Ssi5). Despite their high activity due to their location in the subduction zone, the declustering method tended to remove a significant proportion of their small events, leading to a reduction in the *b-value* in the processed catalog [35,37]. This reduction pattern in the *b-value* introduced a deviation in the recurrence rate, resulting in variability in the calculated accelerations, and, ultimately, increasing the CV for these zones.

For zones like Panama's volcanic arc (P5; P6) and the interface zones of Guatemala (Gsi9) and the Gulf of Fonseca (Nsi15), their high variability was mainly due to their lack of records for low-magnitude earthquakes. Even when the best completeness magnitude (Mc) was selected for the *b-value* fitting method, the lack of small earthquake records could affect the maximum likelihood fitting method, complicating the weighting of these magnitudes and resulting in discrepancies with the least squares method. This impacted the acceleration calculations for these zones.

In the inslab zones of the transition zone between Costa Rica and Panama (Csp15, Csp16), tectonic complexity and the depth at which these earthquakes occurred affected the consistency of the recurrence parameters. Capturing a comprehensive record of all earthquakes in such deep zones is difficult. Additionally, some researchers suggest that declustering methods do not always adequately represent event rates in inslab or deep zones, resulting in models with high variability in seismic acceleration prediction [35,36].

3.4.3. Scaling Relationships for Estimation of Mmax

The maximum possible magnitude (Mmax) calculated from the fault plane geometry, representing in the zone-type source, is conditioned by the scaling relationship applied and the tectonic regime under analysis [51].

An analysis was recently conducted in Central America. Arroyo-Solórzano et al. (2024) [52] defined the scaling relationships for shallow earthquakes of the upper plate in CA based on data from 56 earthquakes. Additionally, they conducted a residual analysis to identify other scaling relationships that fit the observed data and defined a logic tree

to establish the Mmax from different rupture parameters, such as surface rupture length (LRSup), subsurface rupture length (LRSub), width (W), and area (A).

For this study, we focused on scaling relationships using the rupture area (A). For the upper plate regime, we followed the logic tree proposal by Arroyo-Solórzano et al. (2024) [52] and compared the Mmax values given by the scaling relationships from their study with those of Thingbaijam et al. (2017) [53] and Papazachos et al. (2004) [54]. For the interface regime, we compared the results with the relationships proposed by Wells and Coppersmith (1994) [55], Strasser et al. (2010) [56], Allen and Hayes (2017) [57], and Thingbaijam et al. (2017) [53]. Finally, for the inslab regime, we compared only those proposed by Strasser et al. (2010) [56] and Allen and Hayes (2017) [57]. The comparison among the hazard results using different scaling relationships for each tectonic regime was conducted using the coefficient of variation (CV) to assess their spatial variability and whether the application of these relationships significantly affects the accelerations generated across the territory of CA. Figure 5 shows the CV maps for each tectonic regime.

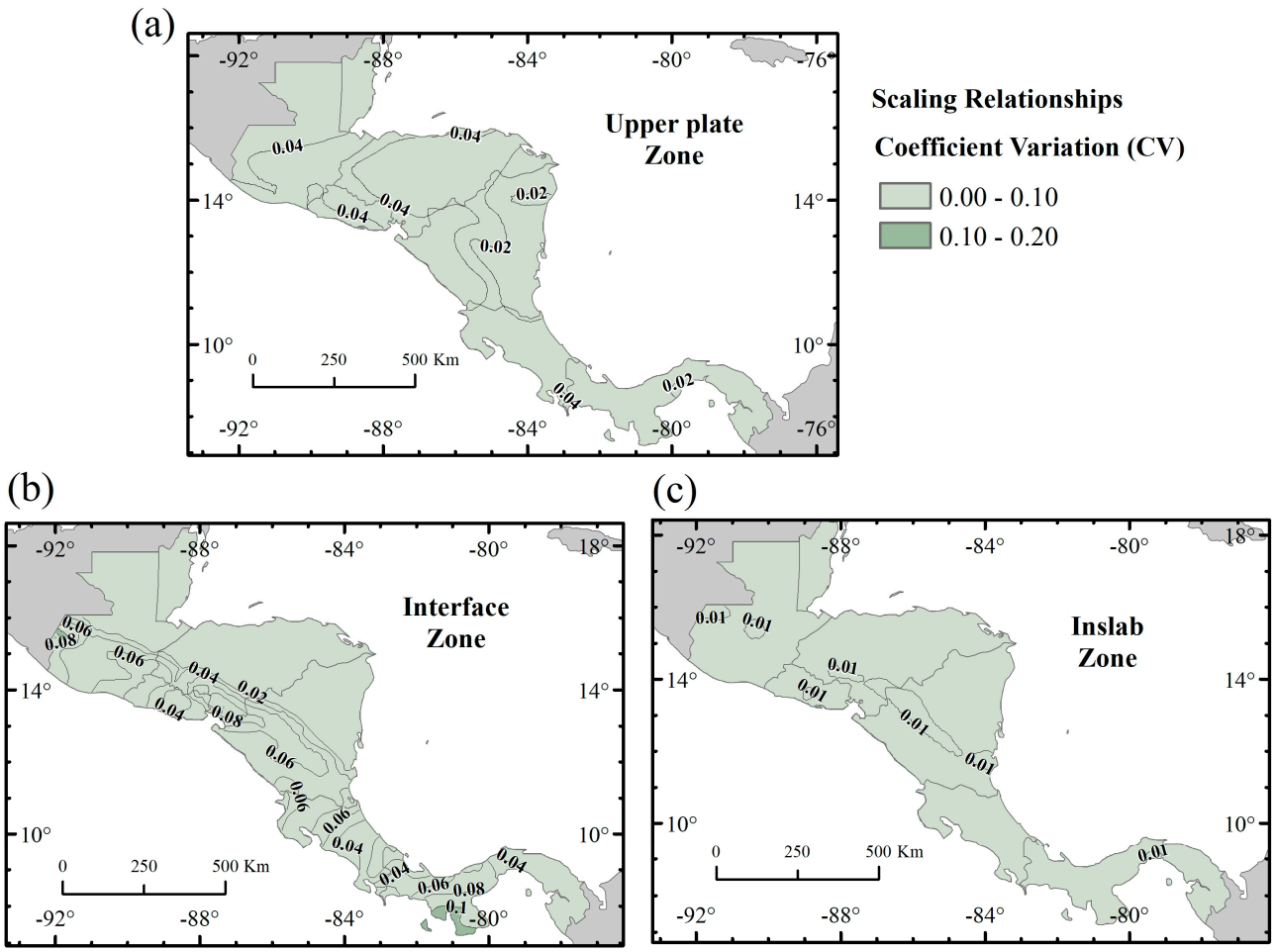


Figure 5. Variability related to scaling relationships for the (**a**) upper plate zone, (**b**) interface zone, and (**c**) inslab zone.

The scaling relationships analyzed in the upper plate regime show no significant variability affecting the seismic hazard calculations because the CV does not exceed 5% (Figure 5a). The interface regime exhibits the greatest data variability, notably in the west of Guatemala and the southern region of the Panama (Azuero Peninsula), with a CV value of up to 10% (Figure 5b). Finally, in the inslab regime, there is no apparent variability according to the spatial distribution of the CV as it does not exceed 1% (Figure 5c).

In general, for the upper plate and inslab regimes, the selected scaling relationships were more consistent and suitable for the analyzed tectonic contexts, which reduced the variability in the Mmax estimations. For example, the relationships developed by Arroyo-Solórzano et al. (2024) [52] focused on regional data from Central America, which minimized variability compared to global relationships such as those proposed by Papazachos (2004) [54] and Thingbajam et al. (2017) [53]. For the inslab regime, the scaling relationships of Allen and Hayes (2017) [57] and Strasser (2010) [56] were specifically designed for subduction seismic events, capturing the characteristics of the deep ruptures typical of subduction earthquakes.

For the interface regime, notable variations can be observed, probably due to the inclusion of multiple scaling relationships that were calibrated with different data and that focus on distinct aspects. The Wells and Coppersmith (1994) [55] relationships are based primarily on data from continental faults, and while they are widely used, they may not fully represent the behavior of subduction zones. Strasser et al. (2010) [56] and Allen and Hayes (2017) [57] focus on subduction earthquakes and are better suited for the interface regime, especially in the Central American region. However, Thingbajam (2017) [53] provides a global scaling relationship that covers a wide variety of tectonic regimes, such as continental faults and subduction zones, meaning their scaling relationship is fitted to global averages as in Wells and Coppersmith (1994) [55].

3.4.4. Ground Motion Models (GMMs)

The selected GMMs were compared using the coefficient of variation (CV). Figure 6 shows the CV maps for the results obtained with the GMMs considered for each tectonic regime.

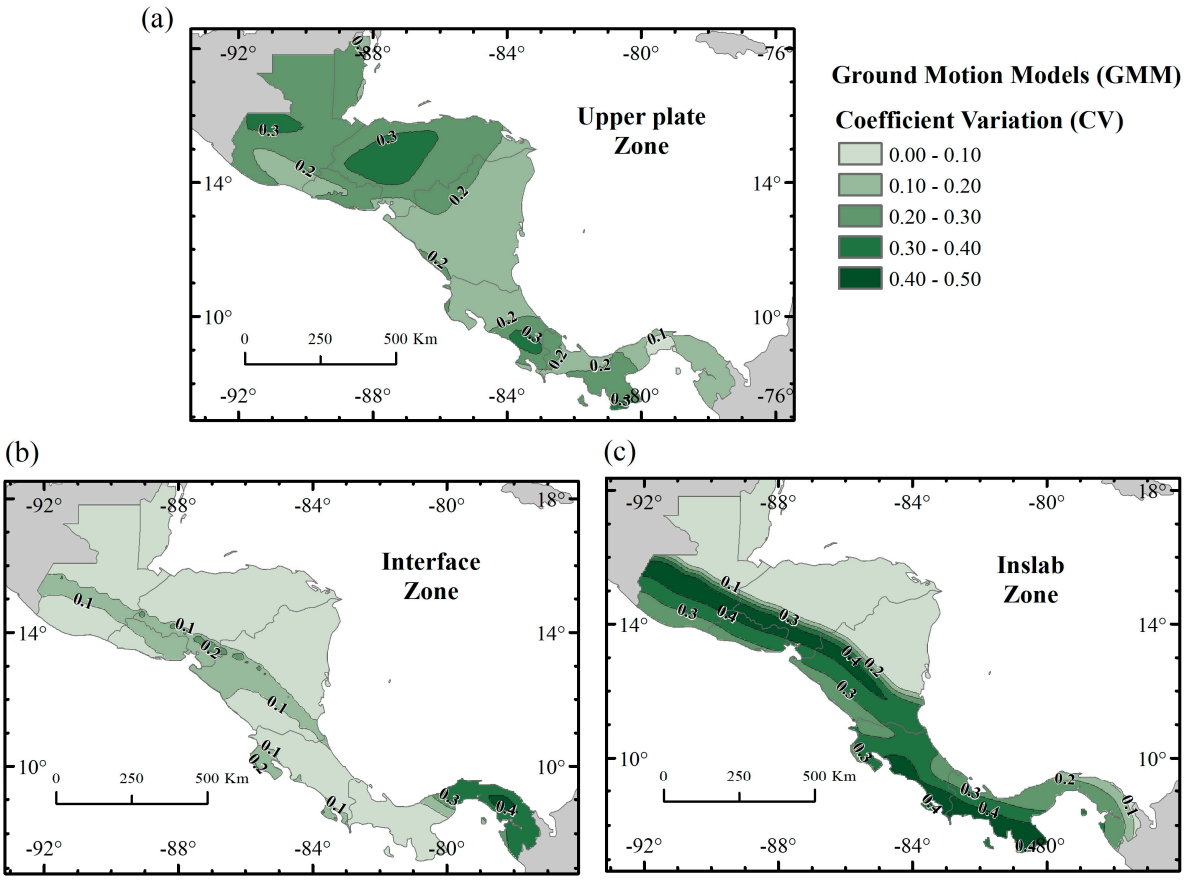


Figure 6. Variability related to GMMs for the (**a**) upper plate zone, (**b**) interface zone and (**c**) inslab zone.

Due to the fact that the GMMs present the greatest variability (Figure 6), we conducted an analysis complementary to the CV, which consisted of studying the variations in accelerations predicted by different GMMs along certain profiles drawn in the CA region. Figure 7 shows the profiles for the upper plate zones and Figure 8 shows the profiles for the interface and inslab zones.

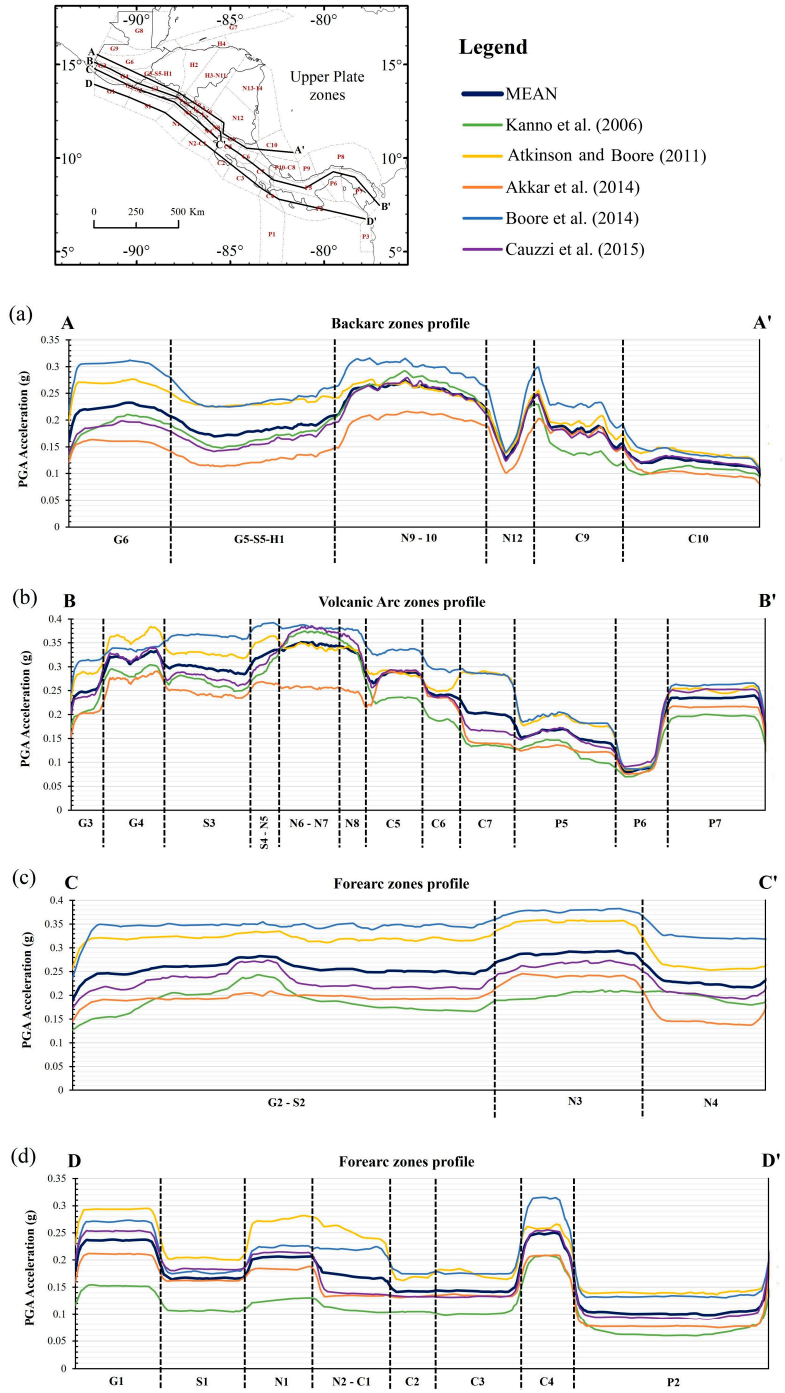


Figure 7. PGA values provided by different GMMs along the profiles drawn for the upper plate zones in (**a**) Backarc, (**b**) volcanic arc, (**c**) middle Forearc, and (**d**) ocean Forearc zones as proposed by Alvarado et al. (2017) [12]. The nomenclature corresponds to the zones represented in Figure 3 and the vertical dashed lines represent the limits of each seismic zone. The GMMs used in this analysis were Kanno et al. (2006) [22], Atkinson and Boore (2011) [23], Akkar et al. (2014) [24], Boore et al. (2014) [25], and Cauzzi et al. (2015) [26].

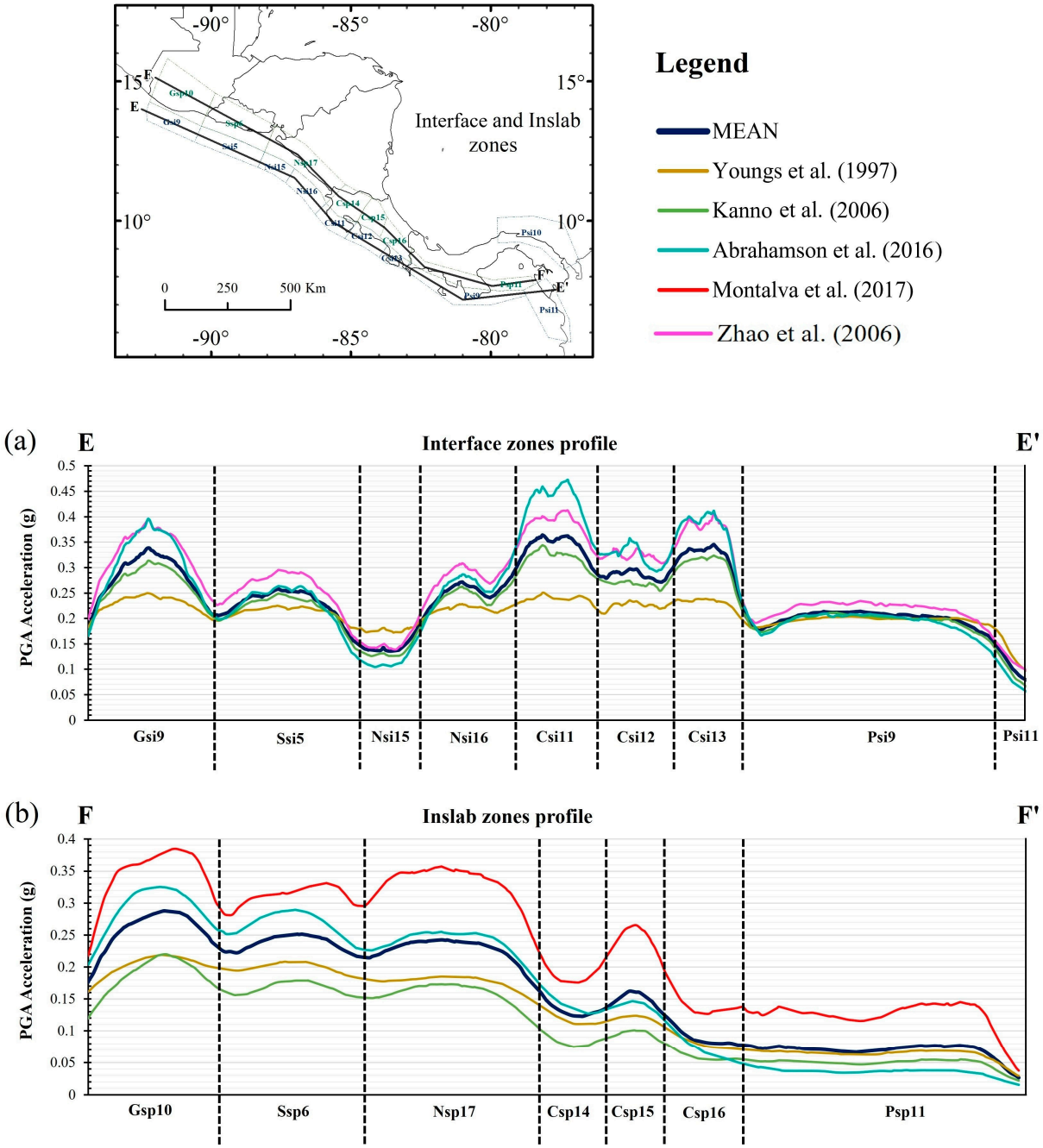


Figure 8. PGA values provided by different GMMs along the profiles drawn for subduction zones in the (**a**) interface zones and (**b**) inslab zones as proposed by Alvarado et al. (2017) [12]. The nomenclature corresponds to the zones represented in Figure 3 and the vertical dashed lines represent the limits of each seismic zone. The GMMs used in this analysis were Youngs et al. (1997) [27], Kanno et al. (2006) [22], Zhao et al. (2006) [28], Abrahamson et al. (2016) [29], and Montalva et al. (2017) [30].

In the upper plate regime, high CV values (CV > 0.30) are observed in certain Backarc zones of Guatemala and Honduras (G6; G5-S5-H1), the volcanic arc of Costa Rica (C7), and the Forearc of Panama (P2) (Figure 6a). This dispersion is also evident in the Backarc zone profile, where in the cases of zones G6 and G5-S5-H1, the models by Atkinson and Boore (2011) [23] and Boore et al. (2014) [25] tend to estimate high accelerations compared to the mean, while the model by Akkar et al. (2014) [24] tends to slightly underestimate them (Figure 7a). For the remaining Backarc zones (N9-10; N12; C9; C10), the GMMs tend to align more closely with the mean, progressively reducing variability to within the range of

0.10–0.20 CV (Figure 6a). Notably, the model by Cauzzi et al. (2015) [26] is that which best aligns with the mean, proving stable for the Backarc zones, followed by the Kanno et al. (2006) [22] model, which slightly underestimates accelerations in some zones (Figure 7a).

For the volcanic arc, the contrast between the profiles and the CV map is notable in zones such as G3, G4, S3, N6-7, C5, and particularly C7, where the acceleration behavior in these volcanic seismic zones tends to produce high dispersion values (Figures 6a and 7b). The models by Boore et al. (2014) [25] and Atkinson and Boore (2011) [23] tend to overestimate accelerations in these zones, particularly in G3, S3, and C7. Conversely, the model by Cauzzi et al. (2015) [26] aligns better with the average accelerations in most of these zones (Figure 7b). Meanwhile, the models by Kanno et al. (2006) [22] and Akkar et al. (2014) [24] slightly underestimate accelerations, though Akkar et al. (2014) [24] generally stabilizes more effectively across most seismic zones (Figure 7b).

For the Forearc zones, particularly those near the Pacific coast, all GMMs show evident dispersion (Figure 7c). This variability is reflected in the map, with CV values around 0.2–0.3 along the coasts of Guatemala, El Salvador, and Nicaragua (Figure 6a). However, in the Forearc zones associated with the Mid-American Trench (MAT), the models by Cauzzi et al. (2015) [26] and Akkar et al. (2014) [24] tend to align more closely with the mean, making these models suitable for these Forearc zones (Figure 7d). In contrast, the models by Boore et al. (2014) [25] and Atkinson and Boore (2011) [23] tend towards slight overestimation in zones such as G1, N1, N2-C1, C4, and P2 (Figure 7d).

In the interface regime, most of the region exhibits relatively low variations (CV < 0.20) (Figure 6b). This aligns with the acceleration profile, where most GMMs fit well with the data mean (Figure 8a). However, zones like Csi11, Csi12, and Csi13 show high dispersion, possibly due to the complexity in the subduction geometry for these areas where the slab is a flat plate with shorter emplacement depths (Figure 8a) [13,19]. The overall behavior of the GMMs of Youngs et al. (1997) [27] and Kanno et al. (2006) [22] tends towards underestimation for the abovementioned zones as these are conservative models, although they stabilize with the models by Abrahamson et al. (2016) [29] and Zhao et al. (2006) [28], which slightly overestimate the accelerations for these interface zones of Costa Rica (Figure 8a).

Finally, the inslab regime presents the highest variations across most of the region due to its deep subduction geometry (Figure 6c). On the one hand, the model by Montalva et al. (2017) [30] shows significant overestimation across all seismic zones, attributed to its calibration for the deep subduction in Chile. On the other hand, the model by Abrahamson et al. (2016) [29] offers a more balanced fit, capturing variations without excessive accelerations and aligning better with the mean in various inslab zones (Figure 8b). The models by Youngs et al. (2017) [27] and Kanno et al. (2006) [22] present slightly low accelerations in deeper subduction zones (Gsp10; Ssp6; Nsp17) (Figure 8b). For a more detailed analysis of the accelerations produced by each of the GMM analyzed, refer to the Supplementary Materials that accompany this article.

3.5. Logic Tree Proposal

We propose a logic tree composed of four nodes related to the methods for defining the aforementioned input parameters: declustering, fitting methods, scaling relationships, and GMMs. At each node, we consider different branches, and the weight for each one is derived from the sensitivity analysis conducted.

As discussed in the previous section, regardless of the declustering method or the *b-value* fitting method, these do not strongly influence the predicted acceleration calculations for Central America. Specific exceptions exist in certain seismic zones where the

declustering and fitting methods are influenced by the completeness of the earthquake catalog derived from the detection level of the corresponding seismic networks [16].

To assign weights to these methods in the logic tree, the approach developed by Gurjar and Basu (2022) [2] is proposed. Following this approach, we estimated the predicted seismic rates [$\dot{N}(m)_{pred}$] using the maximum likelihood (bML) and least squares (bLS) fitting method. Finally, we calculated the mean squared error (MSE) and the root mean squared error (RMSE) of the observed and predicted data starting from the completeness magnitude (Mc).

Gurjar and Basu (2022) [2] established that the weights for the logic tree are inversely proportional to the mean squared error (MSE) of all analyzed seismic zones. To achieve this, the MSEs of all seismic zones were plotted according to the declustering method and the fitting method used in the recurrence models. Subsequently, the errors were fitted to a line from the origin, and finally, the equations by Gurjar and Basu (2022) [2] were applied to assign the weights in the logic tree. For more details, refer to the Supplementary Materials that accompany this article.

Regarding the scaling relationships, for the upper plate regime, we used the weights proposed by Arroyo-Solórzano et al. (2024) [52]. For the interface regime, a higher weight was assigned to the models by Strasser et al. (2010) [56] and Allen and Hayes (2017) [57], as they were specifically calibrated for this tectonic regime and based on Central American data, followed by a smaller weight for the model by Thingbaijam et al. (2017) [53]. Finally, for the inslab regime, equal weight was assigned to both models since the variability was insignificant and less than 1% (Figure 5c).

The structure of the proposed logic tree for GMMs was based on the combined analysis of the profiles and CV maps for each tectonic regime. In the upper plate regime, Cauzzi et al. (2015) [26] was selected as the primary model with a higher weight because it achieves a balanced fit across nearly all seismic zones in the Backarc, volcanic arc, and Forearc, aligning well with the mean in zones of both high and low acceleration. Boore et al. (2014) [25] and Akkar et al. (2014) [24] each received the same weight and were selected because they could also provide a balanced fit for some seismic zones, avoiding overestimation or underestimation of the accelerations. Kanno et al. (2006) [22] was not included in the logic tree for the upper plate due to its tendency to underestimate in volcanic zones and its lack of fit with the attenuation conditions in most seismic zones of the upper plate regime. Similarly, Atkinson and Boore (2011) [23] model was excluded due to its tendency to overestimate accelerations in most upper plate zones.

In the interface regime, equal weight was assigned to Kanno et al. (2006) [22], Zhao et al. (2006) [28], Abrahamson et al. (2016) [29], and Youngs et al. (1997) [27]. This balanced choice reflects the significant dispersion observed in the CV and the need to integrate moderate and conservative models.

In the inslab regime, Abrahamson et al. (2016) [29] received a higher weight due to its ability to capture variability in deep subduction conditions without the overestimations observed in other models. The model by Kanno et al. (2006) [22] also received significant weight, acting as a conservative model useful for representing zones with lower acceleration. Finally, the model by Youngs et al. (1997) [27], with a lower weight, complemented the logic tree by providing an additional perspective in areas where attenuation was more pronounced, which is essential to fully capture the variability of the inslab zones. Montalva et al. (2017) [30] model was excluded due to its tendency to overestimate the accelerations in all inslab zones. Figure 9 shows the proposed logic tree based on this analysis.

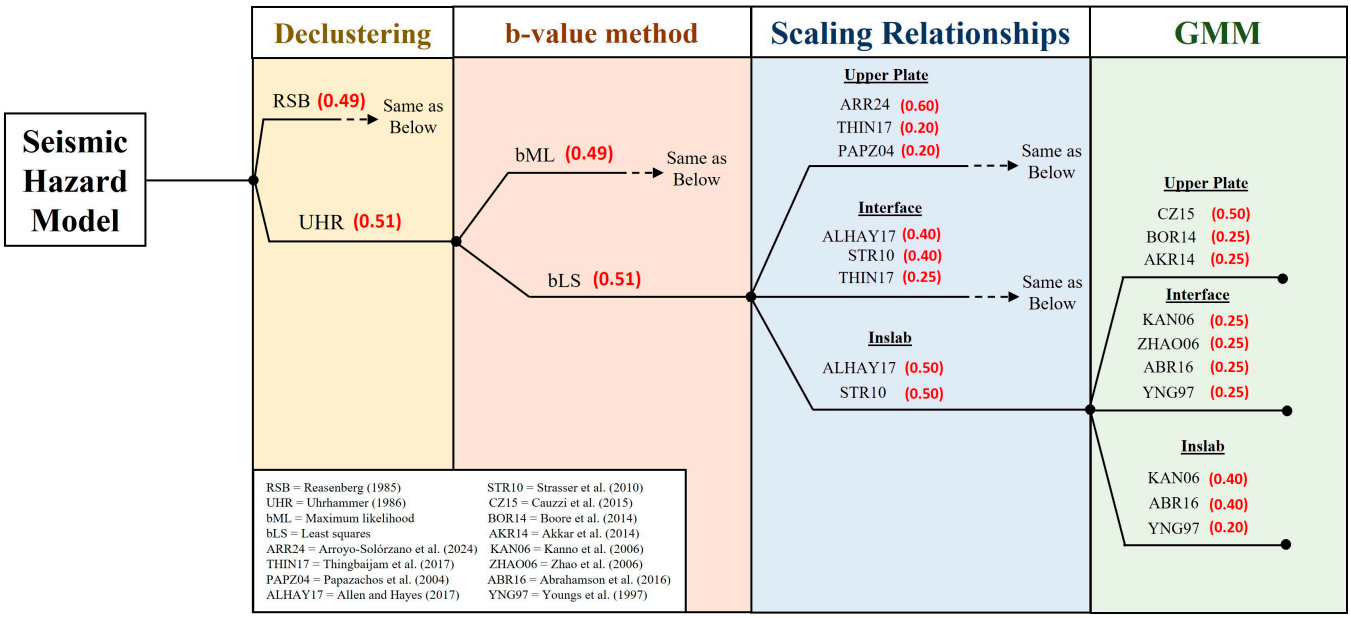


Figure 9. Logic tree proposed for seismic hazard assessments in Central America. RSB—Reasenberg (1985) [38], UHR—Uhrhammer (1986) [40], bML—maximum likelihood fitting method, bLS—least squares fitting method, ARR24—Arroyo-Solórzano et al. (2024) [52], THIN17—Thingbaijam et al. (2017) [53], PAPZ04—Papazachos et al. (2004) [54], STR10—Strasser et al. (2010) [56], ALHAY17—Allen and Hayes (2017) [57], CZ15—Cauzzi et al. (2015) [26], BOR14—Boore et al. (2014) [25], AKR14—Akkar et al. (2014) [24], KAN06—Kanno et al. (2006) [22], ZHAO06—Zhao et al. (2006) [28], ABR16—Abrahamson et al. (2016) [29], YNG97—Youngs et al. (1997) [27].

4. Results

Based on the proposed logic tree, a seismic hazard map for Central America was generated in the form of a spectral ordinate of PGA for return periods of 475 years. For this purpose, we used the OpenQuake program from the Global Earthquake Model (GEM) to conduct seismic hazard calculations [46,47]. The hazard map is shown in Figure 10.

The seismic hazard map for Central America uniformly distributes accelerations across the involved countries, eliminating boundary conditions between them. In general terms, moderate to high accelerations can be observed along the Central American volcanic arc, where the highest accelerations in seismic zones are found in Guatemala (G4), Nicaragua (N6-7), and Costa Rica (C6; C7), with ranges between 0.6 g and 0.7 g (Figure 10). Additionally, the Central Costa Rica Deformed Belt (CCRDB) (P10-C8) shows relatively high accelerations (0.5 g–0.6 g) due to an increased rate of seismic activity recorded in the regional earthquake catalog, which highlights this area (Figure 10).

Furthermore, implementing the seismic zonation by Alvarado et al. (2017) [12] improved the adjustment of the depths in the interface and inslab seismic zones, resulting in a more realistic representation of the accelerations induced by the dip angle variations along the Mid-American Trench (MAT). This adjustment produced higher accelerations along the coasts of Guatemala, El Salvador, Nicaragua, and Costa Rica, where values reached between 0.6 g and 0.9 g (Figure 10). Additionally, this zonation refined the geometry of the South Panama Deformed Belt (SPDB), leading to more realistic acceleration values in the Azuero Peninsula, reaching up to 0.5 g (Figure 10).

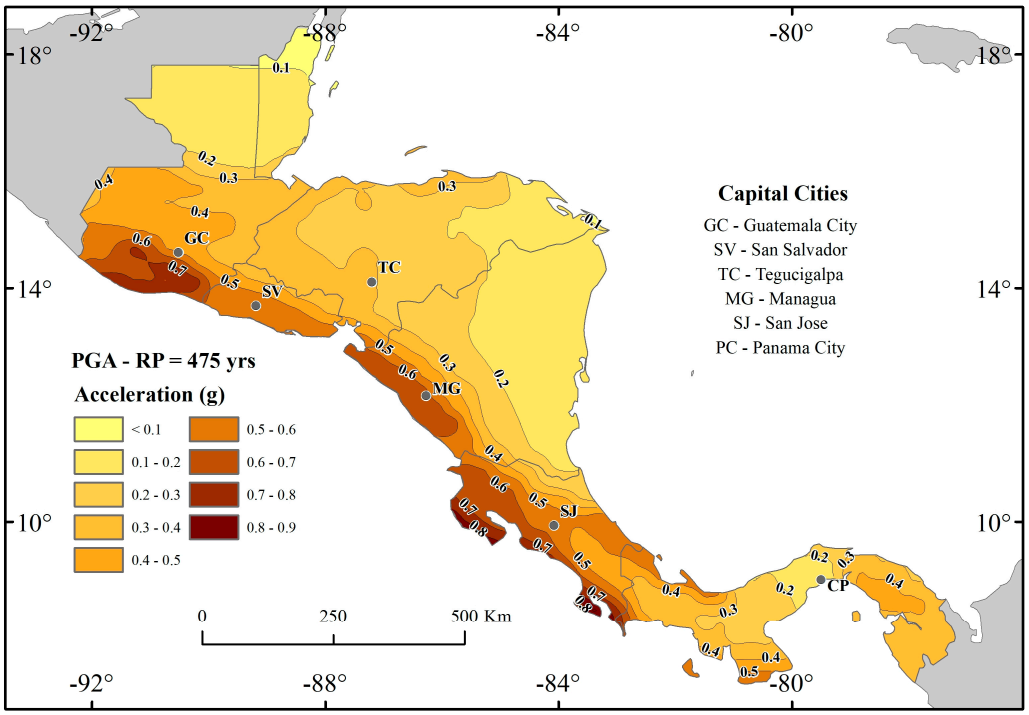


Figure 10. Seismic hazard map for Central America for PGA and return period of 475 years on rock conditions (Vs_{30} = 760 m/s).

5. Discussion and Conclusions

A sensitivity analysis of the parameters and methods interacting in seismic hazard calculations provided better control of epistemic uncertainties, selecting the optimal parameters and methods for the tectonic characteristics of Central America. This sensitivity analysis focused on evaluating the impact on the results of the following inputs and methods integrated into seismic hazard calculations in classical zoned methods: (1) declustering methods for identifying fore and aftershocks, (2) methods for fitting the recurrence models (*b-value* and *a-value*), (3) scaling relationships for estimating Mmax, and (4) the application of different ground motion models (GMMs).

Two statistical approaches were used for the sensitivity analysis. The first consists of calculating the coefficient of variation (CV) of the results, achieved through different calculation options, which indicates the degree of variability in the hazard results depending on the analyzed input data and models. The coefficient of variation (CV) is a particularly useful statistical parameter when identifying specific areas where significant variability may impact the final seismic hazard assessment, allowing researchers to identify causes for these variations and ways to manage them to reduce epistemic uncertainties.

The second approach is based on statistical methods that determine the mean squared error (MSE) and root mean squared error (RMSE) of the observed and predicted data. Metrics like the MSE and RMSE are useful for selecting the most appropriate predictive model that fits the observed data, aiding in the more precise assignment of weights within the logic tree [2].

These approaches were carried out to evaluate the impact of parameters and models in the successive phases of hazard calculation using classical zoned methods, which consider the seismicity randomly distributed within each seismic zone. In a first step, these methods require the aftershocks and premonitors to be identified and eliminated, thus considering only main events, for which this hypothesis of randomness can be assumed. For this purpose, two methods were used: (1) the Reasenberg (1985) [38] declustering method (RSB) and (2) Uhrhammer (1986) [40] declustering (UHR). In a second step, a recurrence model

for the seismicity of each seismic source must be estimated. We adopted the recurrence model proposed by Gutenberg and Richter (1944) [48] and we used two methods to fit the model: (1) least squares (bLS) and (2) maximum likelihood (bML).

A joint sensitivity analysis was performed for the four combinations of the declustering–fitting methods: (1) RSB-bLS, (2) RSB-bML, (3) UHR-bLS, and (4) UHR-bML. According to the results obtained, the low CV value (CV < 0.10) in most areas of Central America indicates the low impact of these methods on the hazard results. On the contrary, high consistency was found in the accelerations calculated under the different combinations of declustering and fitting methods for the recurrence model. This indicates the stability of the accelerations predicted by the different combinations regardless of the method used in this calculation phase.

The third aspect analyzed was the impact of the scaling relationships to obtain the Mmax of the zones in the final hazard results. In this case, the CV values did not exceed 5% in the upper plate regime, showing that there is no significant variability in the hazard results depending on the scaling relationship used, or ultimately on the Mmax corresponding to each zone. The interface regime exhibited the greatest data variability, notably in the west of Guatemala and the southern region of Panama (Azuero Peninsula), with a CV value of up to 10%. Finally, in the inslab regime, there was no apparent variability according to the spatial distribution of the CV, as it did not exceed 1%. This may be due to the fact that the available relationships included in this analysis were more suitable to upper plate and inslab contexts than to the interface regimes. In any case, it can be concluded from the analysis that these scaling relationships have a low impact on the hazard results.

The final issue addressed in the sensitivity analysis was the impact of GMMs. These models had the greatest impact on the hazard results among all the variables analyzed. In the upper plate regime, high CV values (CV > 0.30) were observed in certain Backarc zones of Guatemala and Honduras, the volcanic arc of Costa Rica, and the Forearc of Panama. This dispersion was also evident in some Backarc zones, while in others the variability was reduced with a lower dispersion between the results given by the different models, with CV values in the range of 0.10–0.20.

For the Forearc zones, particularly those near the Pacific coast, all GMMs showed evident dispersion. This variability is reflected in the map, with CV values around 0.2–0.3 along the coasts of Guatemala, El Salvador, and Nicaragua. However, in the Forearc zones associated with the Mid-American Trench (MAT), the models by Cauzzi et al. (2015) [26] and Akkar et al. (2014) [24] tended to align more closely with the mean, making these models more suitable for these Forearc zones. In contrast, the models by Boore et al. (2014) [25] and Atkinson and Boore (2011) [23] tended to slightly overestimate.

In the interface regime, most of the region exhibited relatively low variations (CV < 0.20). Most GMMs fit well with the data mean. However, the zones of Costa Rica showed high dispersion, possibly due to the complexity in the subduction geometry for these areas where the slab is a flat plate with shorter emplacement depths.

Finally, the inslab regime presented the highest variations across most of the region due to its deep subduction geometry. On the one hand, the model by Montalva et al. (2017) [30] showed significant overestimation across all seismic zones, which can be attributed to its calibration for the deep subduction in Chile. On the other hand, the model by Abrahamson et al. (2016) [29] offered a more balanced fit, aligning better with the mean in various inslab zones.

The sensitivity analysis concluded with the proposal for a logic tree composed of four nodes related to the methods for defining the input parameters: declustering methods, methods for fitting of the Gutenberg–Richter model, scaling relationships, and GMMs. At each node, we considered different branches, and the weight for each one was derived

from the sensitivity analysis carried out, particularly taking into account the CV values, the mean squared error (MSE), and the root mean squared error (RMSE) of the observed and predicted data.

Using this logic tree, a new regional hazard calculation for CA was performed, and a map was generated to update the one published in 2012 in the frame of the RESIS II project [3]. The main novelties included in this new map are the implementation of the seismic zonation by Alvarado et al. (2017) [12], the update of the regional earthquake catalog with data from local agencies up to 2020 [16], the implementation of scaling relationships specific to Central America [52], and the control of epistemic uncertainties through a logic tree proposal derived from a sensitivity analysis of the model parameters in the hazard results.

When comparing the seismic hazard map from the RESIS II project [3] with the one generated in this study through a map representing the ratio of accelerations between this study and that of RESIS II, we can identify specific areas where accelerations have increased or decreased (Figure 11). Overall, there is a general increase of 10% to 50% in accelerations compared to the RESIS II map. This increase is largely attributable to the expanded records in the regional earthquake catalog, improvements in recurrence models, and the use of seismic zonation by Alvarado et al. (2017) [12]. Otherwise, some areas remain stable across both seismic hazard maps, showing that the results are robust in these areas and are hardly affected by the variations included in this new study (Figure 11).

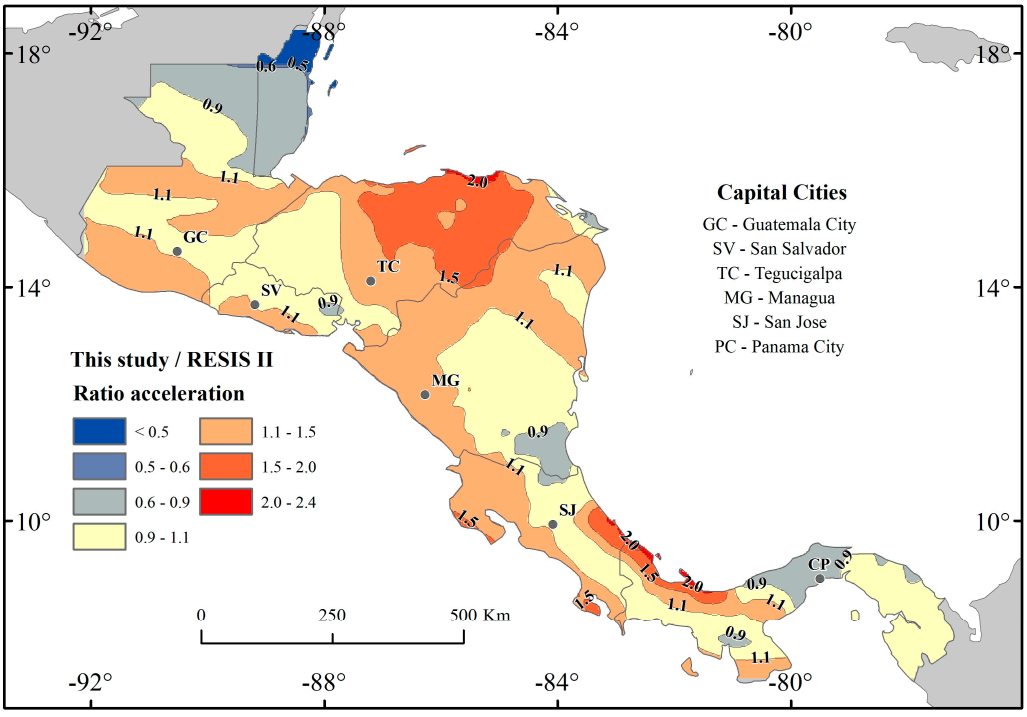


Figure 11. Map showing the ratio of acceleration in this study and the RESIS II project [3].

Additionally, areas of interest can be observed where the increase in acceleration values exceeds 50% compared to those reflected in the previous RESIS II map, particularly in northern Honduras and the Northern Costa Rica Deformed Belt (CCRDB). This increase is attributed to the improved capture of seismic events in these areas, where these events have been incorporated into the updated regional earthquake catalog, significantly enhancing the parameters of the seismic source [16]. Likewise, small areas with a reduction in accelerations of up to almost 30% can be appreciated, especially in northern Guatemala and central Panama. This reduction is mainly due to the seismic zonation by Alvarado et al.

(2017) [12], where modifications and improvements in the definition of seismic zones are more closely aligned with the tectonic behavior occurring in these areas.

In conclusion, this sensitivity analysis conducted on the parameters and methods involved in seismic hazard calculations has provided improved control over epistemic uncertainties, leading to a logic tree proposal based on the results of the analysis, both with regard to CV values as well as other statistical parameters, such as the MSE and RMSE.

This rigorous analysis has led to a seismic hazard map that can be considered an update to the RESIS II hazard map [3], since it enhances the representation of accelerations in the region by incorporating new seismic information from the latest studies for Central America. This includes the seismic zonation by Alvarado et al. (2017) [12] and the scaling relationships for the upper plate regime by Arroyo-Solórzano et al. (2024) [52], which are specific to this region.

Supplementary Materials: The following supporting information can be downloaded at https://www.mdpi.com/article/10.3390/geosciences15010004/s1.

Author Contributions: Conceptualization, C.G.-C. and B.B.; methodology, C.G.-C., M.A.-S., A.R.-M. and B.B; software, C.G.-C.; validation, M.A.-S., A.R.-M. and B.B.; formal analysis, C.G.-C., A.R.-M., M.A.-S. and B.B.; writing—original draft preparation, C.G.-C.; writing—review and editing, M.A.-S., A.R.-M. and B.B.; supervision, A.R.-M. and B.B. All authors have read and agreed to the published version of the manuscript.

Funding: This research was funded by the KUK-APHÁN project (RTI2018-094827-B-C21/C22), the Ministerio de Ciencia, Innovación y Universidades del Gobierno de España, and MCIN/AEI/10.13039/501100011033, and, if applicable, by "FEDER A way to do Europe".

Data Availability Statement: The original contributions presented in the study are included in the article/Supplementary Material; further inquiries can be directed to the corresponding author.

Acknowledgments: The authors would like to acknowledge all their colleagues involved in the KUK-AHPÁN project from Central America.

Conflicts of Interest: The authors declare no conflicts of interest.

References

1. Ghods, B.; Rofooei, F.R. Addressing the Epistemic Uncertainty in Seismic Hazard Analysis as a Basis for Seismic Design by Emphasizing the Knowledge Aspects and Utilizing Imprecise Probabilities. *Bull. Earthq. Eng.* **2022**, *20*, 741–764. [CrossRef]
2. Gurjar, N.; Basu, D. Epistemic Uncertainty in PSHA and Seismic Hazard Characterization Using the Logic Tree Approach: Part I, Developing the Framework. *Pure Appl. Geophys.* **2022**, *179*, 3647–3676. [CrossRef]
3. Benito, M.B.; Lindholm, C.; Camacho, E.; Climent, A.; Marroquín, G.; Molina, E.; Rojas, W.; Escobar, J.J.; Talavera, E.; Alvarado, G.E.; et al. A New Evaluation of Seismic Hazard for the Central America Region. *Bull. Seismol. Soc. Am.* **2012**, *102*, 504–523. [CrossRef]
4. Peirce, C.; Grevemeyer, I.; Hayman, N.W.; Van Avendonk, H.J.A. Active Ocean-Continent Transform Margins: Seismic Investigation of the Cayman Trough-Swan Island Ridge-Transform Intersection. *Geophys. J. Int.* **2022**, *229*, 1604–1627. [CrossRef]
5. Finch, R.C.; Ritchie, A.W. The Guayape Fault System, Honduras, Central America. *J. S. Am. Earth Sci.* **1991**, *4*, 43–60. [CrossRef]
6. Garnier, B.; Tikoff, B.; Flores, O.; Jicha, B.; DeMets, C.; Cosenza-Muralles, B.; Hernandez, W.; Greene, D. Deformation in Western Guatemala Associated With the NAFCA (North America-Central American Forearc-Caribbean) Triple Junction: Neotectonic Strain Localization Into the Guatemala City Graben. *Tectonics* **2022**, *41*, 1–34. [CrossRef]
7. Garnier, B.; Tikoff, B.; Flores, O.; Jicha, B.; DeMets, C.; Cosenza-Muralles, B.; Hernandez, D.; Marroquin, G.; Mixco, L.; Hernandez, W. An Integrated Structural and GPS Study of the Jalpatagua Fault, Southeastern Guatemala. *Geosphere* **2021**, *17*, 201–225. [CrossRef]
8. Staller, A.; Martínez-Díaz, J.J.; Benito, B.; Alonso-Henar, J.; Hernández, D.; Hernández-Rey, R.; Díaz, M. Present-Day Crustal Deformation along the El Salvador Fault Zone from ZFESNet GPS Network. *Tectonophysics* **2016**, *670*, 66–81. [CrossRef]
9. Martínez-Díaz, J.J.; Álvarez-Gómez, J.A.; Staller, A.; Alonso-Henar, J.; Canora, C.; Insúa-Arévalo, J.M.; Tsige, M.; Villamor, P.; Herrero-Barbero, P.; Hernández-Moreno, C.; et al. Active Faults of El Salvador. *J. S. Am. Earth Sci.* **2021**, *105*, 1–20. [CrossRef]

10. Funk, J.; Mann, P.; McIntosh, K.; Stephens, J. Cenozoic Tectonics of the Nicaraguan Depression, Nicaragua, and Median Trough, El Salvador, Based on Seismic-Reflection Profiling and Remote-Sensing Data. *Bull. Geol. Soc. Am.* **2009**, *121*, 1491–1521. [CrossRef]
11. DeMets, C.; Gordon, R.G.; Argus, D.F. Geologically Current Plate Motions. *Geophys. J. Int.* **2010**, *181*, 1–80. [CrossRef]
12. Alvarado, G.E.; Benito, B.; Staller, A.; Climent, Á.; Camacho, E.; Rojas, W.; Marroquín, G.; Molina, E.; Talavera, J.E.; Martínez-Cuevas, S.; et al. The New Central American Seismic Hazard Zonation: Mutual Consensus Based on up to Day Seismotectonic Framework. *Tectonophysics* **2017**, *721*, 462–476. [CrossRef]
13. Lücke, O.H.; Arroyo, I.G. Density Structure and Geometry of the Costa Rican Subduction Zone from 3-D Gravity Modeling and Local Earthquake Data. *Solid Earth* **2015**, *6*, 1169–1183. [CrossRef]
14. Westbrook, G.K.; Hardy, N.C.; Heath, R.P. *Structure and Tectonics of the Panama-Nazca Plate Boundary*; GSA Special Papers; Geological Society of America: Boulder, CO, USA, 1995; Volume 295, pp. 91–110.
15. Carvajal-Arenas, L.C.; Mann, P. Western Caribbean Intraplate Deformation: Defining a Continuous and Active Microplate Boundary along the San Andres Rift and Hess Escarpment Fault Zone, Colombian Caribbean Sea. *Am. Assoc. Pet. Geol. Bull.* **2018**, *102*, 1523–1563. [CrossRef]
16. Gamboa-Canté, C.; Arroyo-Solórzano, M.; Benito, B.; Aguilar, J.; Arroyo, I.G.; Camacho-Astigarrabia, E.; Castro, D.; Flores, O.; Linkimer, L.; Marroquin, M.G.; et al. Seismicity in Central America (1520–2020) and Earthquake Catalog Compilation for Seismic Hazard Assessments. *Bull. Earthq. Eng.* **2024**, *22*, 7201–7234. [CrossRef]
17. Stepp, J.C. Analysis of Completeness of the Earthquake Sample in the Puget Sound Area and Its Effect on Statistical Estimates of Earthquake Hazard. In Proceedings of the International Conference on Microzonation, Boulder, CO, USA, 1972; pp. 897–910.
18. Mixco Durán, L.E. *Evaluación Probabilística de Amenaza Sísmica de El Salvador*; Ministerio de Medio Ambiente y Recursos Naturales, Dirección General del Observatorio Ambiental: San Salvador, El Salvador, 2020.
19. Hidalgo-Leiva, D.A.; Linkimer, L.; Arroyo, I.G.; Arroyo-Solórzano, M.; Piedra, R.; Climent, A.; Díaz, V.S.; Esquivel, L.C.; Alvarado, G.E.; Castillo, R.; et al. The 2022 Seismic Hazard Model for Costa Rica. *Bull. Seismol. Soc. Am.* **2023**, *113*, 23–40. [CrossRef]
20. Scherbaum, F.; Delavaud, E.; Riggelsen, C. Model Selection in Seismic Hazard Analysis: An Information-Theoretic Perspective. *Bull. Seismol. Soc. Am.* **2009**, *99*, 3234–3247. [CrossRef]
21. Kale, O.; Akkar, S. A New Procedure for Selecting and Ranking Ground-Motion Prediction Equations (GMPEs): The Euclidean Distance-Based Ranking (EDR) Method. *Bull. Seismol. Soc. Am.* **2013**, *103*, 1069–1084. [CrossRef]
22. Kanno, T.; Narita, A.; Morikawa, N.; Fujiwara, H.; Fukushima, Y. A New Attenuation Relation for Strong Ground Motion in Japan Based on Recorded Data. *Bull. Seismol. Soc. Am.* **2006**, *96*, 879–897. [CrossRef]
23. Atkinson, G.M.; Boore, D.M. Modifications to Existing Ground-Motion Prediction Equations in Light of New Data. *Bull. Seismol. Soc. Am.* **2011**, *101*, 1121–1135. [CrossRef]
24. Akkar, S.; Sandıkkaya, M.A.; Bommer, J.J. Empirical Ground-Motion Models for Point- and Extended-Source Crustal Earthquake Scenarios in Europe and the Middle East. *Bull. Earthq. Eng.* **2014**, *12*, 359–387. [CrossRef]
25. Boore, D.M.; Stewart, J.P.; Seyhan, E.; Atkinson, G.M. NGA-West2 Equations for Predicting PGA, PGV, and 5% Damped PSA for Shallow Crustal Earthquakes. *Earthq. Spectra* **2014**, *30*, 1057–1085. [CrossRef]
26. Cauzzi, C.; Faccioli, E.; Vanini, M.; Bianchini, A. Updated Predictive Equations for Broadband (0.01–10 s) Horizontal Response Spectra and Peak Ground Motions, Based on a Global Dataset of Digital Acceleration Records. *Bull. Earthq. Eng.* **2015**, *13*, 1587–1612. [CrossRef]
27. Youngs, R.R.; Chiou, S.-J.; Silva, W.J.; Humphrey, J.R. Strong Ground Motion Attenuation Relationships for Subduction Zone Earthquakes. *Seismol. Res. Lett.* **1997**, *68*, 58–73. [CrossRef]
28. Zhao, J.X.; Zhang, J.; Asano, A.; Ohno, Y.; Oouchi, T.; Takahashi, T.; Ogawa, H.; Irikura, K.; Thio, H.K.; Somerville, P.G.; et al. Attenuation Relations of Strong Ground Motion in Japan Using Site Classification Based on Predominant Period. *Bull. Seismol. Soc. Am.* **2006**, *96*, 898–913. [CrossRef]
29. Abrahamson, N.; Gregor, N.; Addo, K. BC Hydro Ground Motion Prediction Equations For Subduction Earthquakes. *Earthq. Spectra* **2016**, *32*, 23–44. [CrossRef]
30. Montalva, G.A.; Bastías, N.; Rodriguez-Marek, A. Ground-Motion Prediction Equation for the Chilean Subduction Zone. *Bull. Seismol. Soc. Am.* **2017**, *107*, 901–911. [CrossRef]
31. Lombardi, A.M.; Akinci, A.; Malagnini, L.; Mueller, C.S. Uncertainty Analysis for Seismic Hazard in Northern and Central Italy. *Ann. Geophys.* **2005**, *48*, 853–865. [CrossRef]
32. Gaspar-Escribano, J.M.; Rivas-Medina, A.; Parra, H.; Cabañas, L.; Benito, B.; Ruiz Barajas, S.; Martínez Solares, J.M. Uncertainty Assessment for the Seismic Hazard Map of Spain. *Eng. Geol.* **2015**, *199*, 62–73. [CrossRef]
33. Hamdache, M.; Pelaéz, J.A.P.; Henares, J.; Sawires, R. Seismic Hazard Assessment and Its Uncertainty for the Central Part of Northern Algeria. *Pure Appl. Geophys.* **2022**, *179*, 2083–2118. [CrossRef]
34. Scheingraber, C.; Käser, M. Spatial Seismic Hazard Variation and Adaptive Sampling of Portfolio Location Uncertainty in Probabilistic Seismic Risk Analysis. *Nat. Hazard. Earth Syst. Sci.* **2020**, *20*, 1903–1918. [CrossRef]

35. Mizrahi, L.; Nandan, S.; Wiemer, S. The Effect of Declustering on the Size Distribution of Mainshocks. *Seismol. Res. Lett.* **2021**, *92*, 2333–2342. [CrossRef]
36. Taroni, M.; Akinci, A. Good Practices in PSHA: Declustering, b-Value Estimation, Foreshocks and Aftershocks Inclusion; A Case Study in Italy. *Geophys. J. Int.* **2021**, *224*, 1174–1187. [CrossRef]
37. Perry, M.; Bendick, R. A Comparative Analysis of Five Commonly Implemented Declustering Algorithms. *J. Seism.* **2024**, *28*, 829–842. [CrossRef]
38. Reasenberg, P. Second-Order Moment of Central California Seismicity, 1969–1982. *J. Geophys. Res.* **1985**, *90*, 5479–5495. [CrossRef]
39. Gardner, J.K.; Knopoff, L. Is the Sequence of Earthquakes in Southern California, with Aftershocks Removed, Poissonian? *Bull. Seismol. Soc. Am.* **1974**, *64*, 1363–1367. [CrossRef]
40. Uhrhammer, R.A. Characteristics of Northern and Central California Seismicity. *Earthq. Notes* **1986**, *57*, 21.
41. Garcia-Pelaez, J.; Gee, R.; Styron, R.; Poggi, V. *PSHA Input Model Documentation for Caribbean and Central America (CCA)*; Global Earthquake Model: Pavia, Italy, 2019.
42. Álvarez, L. Nueva Estimación de La Amenaza Sísmica Para Nicaragua. *Rev. Tierra* **2022**, *2*, 1–18.
43. Arroyo-Solórzano, M.; Linkimer, L. Spatial Variability of the B-Value and Seismic Potential in Costa Rica. *Tectonophysics* **2021**, *814*, 1–18. [CrossRef]
44. Wiemer, S. A Software Package to Analyze Seismicity: ZMAP. *Seismol. Res. Lett.* **2001**, *72*, 373–382. [CrossRef]
45. Weatherill, G.; Rodríguez, L.; Pagani, M. The Seismic Hazard Modeller's Toolkit: An Open-Source Library for the Construction of Probabilistic Seismic Hazard Models. In Proceedings of the Second European Conference on Earhquake Engineering and Seismology, Istanbul, Turkey, 25 August 2014; pp. 1–12.
46. Pagani, M.; Monelli, D.; Weatherill, G.; Danciu, L.; Crowley, H.; Silva, V.; Henshaw, P.; Butler, L.; Nastasi, M.; Panzeri, L.; et al. Openquake Engine: An Open Hazard (and Risk) Software for the Global Earthquake Model. *Seismol. Res. Lett.* **2014**, *85*, 692–702. [CrossRef]
47. Silva, V.; Crowley, H.; Pagani, M.; Monelli, D.; Pinho, R. Development of the OpenQuake Engine, the Global Earthquake Model's Open-Source Software for Seismic Risk Assessment. *Nat. Hazards* **2014**, *72*, 1409–1427. [CrossRef]
48. Gutenberg, B.; Richter, C.F. Frequency of Earthquakes in California. *Bull. Seismol. Soc. Am.* **1944**, *34*, 185–188. [CrossRef]
49. Aki, K. Maximum Likelihood Estimate of b in the Formula LogN=a-bM and Its Confidence Limits. *Bull. Earthq. Res. Inst.* **1965**, *43*, 237–239.
50. Weichert, D.H. Estimation of the Earthquake Recurrence Parameters for Unequal Observation Periods for Different Magnitudes. *Bull. Seismol. Soc. Am.* **1980**, *70*, 1337–1346. [CrossRef]
51. Shaw, B.E. Magnitude and Slip Scaling Relations for Fault-Based Seismic Hazard. *Bull. Seismol. Soc. Am.* **2023**, *113*, 924–947. [CrossRef]
52. Arroyo-Solórzano, M.; Belén Benito, M.; Alvarado, G.E.; Climent, A. Empirical Earthquake Source Scaling Relations for Maximum Magnitudes Estimations in Central America. *Bull. Seismol. Soc. Am.* **2024**, *114*, 1539–1567. [CrossRef]
53. Thingbaijam, K.K.S.; Mai, P.M.; Goda, K. New Empirical Earthquake Source-Scaling Laws. *Bull. Seismol. Soc. Am.* **2017**, *107*, 2225–2246. [CrossRef]
54. Papazachos, B.C.; Scordilis, E.M.; Panagiotopoulos, D.G.; Papazachos, C.B.; Karakaisis, G.F. Global Relations between Seismic Fault Parameters and Moment Magnitude of Earthquakes. *Bull. Geol. Soc. Greece* **2004**, *36*, 1482–1489. [CrossRef]
55. Wells, D.L.; Coppersmith, K.J. New Empirical Relationships among Magnitude, Rupture Length, Rupture Width, Rupture Area, and Surface Displacement. *Bull. Seismol. Soc. Am.* **1994**, *84*, 974–1002. [CrossRef]
56. Strasser, F.O.; Arango, M.C.; Bommer, J.J. Scaling of the Source Dimensions of Interface and Intraslab Subduction-Zone Earthquakes with Moment Magnitude. *Seismol. Res. Lett.* **2010**, *81*, 941–950. [CrossRef]
57. Allen, T.I.; Hayes, G.P. Alternative Rupture-Scaling Relationships for Subduction Interface and Other Offshore Environments. *Bull. Seismol. Soc. Am.* **2017**, *107*, 1240–1253. [CrossRef]

Disclaimer/Publisher's Note: The statements, opinions and data contained in all publications are solely those of the individual author(s) and contributor(s) and not of MDPI and/or the editor(s). MDPI and/or the editor(s) disclaim responsibility for any injury to people or property resulting from any ideas, methods, instructions or products referred to in the content.